Investigations of the MceIJ-Catalyzed Posttranslational Modification of the Microcin E492 C-Terminus: Linkage of Ribosomal and Nonribosomal Peptides To Form "Trojan Horse" Antibiotics[†]

Elizabeth M. Nolan and Christopher T. Walsh*

Department of Biological Chemistry and Molecular Pharmacology, Harvard Medical School, Boston, Massachusetts 02115

Received May 6, 2008; Revised Manuscript Received June 7, 2008

ABSTRACT: MceIJ is a two protein complex responsible for attachment of a C-glycosylated and linearized derivative of enterobactin, an iron scavenger (siderophore) and product of nonribosomal peptide synthetase machinery, to the C-terminal serine residue of microcin E492 (MccE492), an 84 aa ribosomal antibiotic peptide produced by *Klebsiella pneumoniae* RYC492. The MceIJ-catalyzed formation of the glycosyl ester linkage between MccE492 and the siderophore requires ATP and Mg(II) as cofactors. This work addresses the ATP utilization, mechanism of C-terminal carboxylate activation, and substrate scope of MceIJ. Formation of the ribosomal peptide−nonribosomal peptide linkage between the MccE492 C-terminal decapeptide and monoglycosylated enterobactin (MGE) requires cleavage of the α,β bond of ATP and formation of a putative peptidyl-CO-AMP intermediate. Attack of the peptidyl-CO-AMP carbonyl by the deprotonated C4′ hydroxyl of the glucose moiety forms a glycosyl ester linkage with release of AMP. Site-directed mutagenesis of the three cysteines and five histidines in MceI to alanines reveals that these residues are not required structurally or catalytically. MceIJ recognizes all glycosylated enterobactin derivatives formed by the MccE492 gene cluster members MceC (*C*-glycosyltransferase) and MceD (esterase) in vitro and a MGE derivative lacking the C6′ hydroxyl moiety. The protein complex also accepts and modifies the C-terminal decapeptide substrate fragments of the structurally related microcins H47, I47, and M. MccE492 C-terminal decapeptides bearing fluorescein and biotin moieties on the N-terminus are also substrates for MceIJ, which provides a route for the chemoenzymatic synthesis of enterobactin conjugates with peptide linkages.

Bacteria produce peptide-based antibiotics to eradicate competing species and survive in the host environment. Many of these secondary metabolites, including penicillin, cephalosporin, and vancomycin, are produced by nonribosomal peptide synthetases (NRPS)[1] whereas others are produced on the ribosome. Microcins constitute a class of ribosomal, low-molecular-weight (<10000 Da), antibiotic peptides that are generated by enterobacteria during periods of nutrient deprivation and stress to kill off their susceptible competitors (*1–3*). The peptides exhibit diverse structural features and mechanisms of action. Several microcins undergo posttranslational modifications that are critical for their physiological function. The peptide backbone of microcin B17, a DNA gyrase inhibitor produced by *Escherichia coli* strains carrying the pMccB17 plasmid, undergoes heterocyclization during maturation (*4–6*). This process creates four thiazole and four oxazole moieties from six glycines, four serines, and four cysteines and rigidifies the peptide backbone. Microcin J25, a 21-residue peptide produced by *E. coli* AY25 harboring the pTUC100 plasmid, is a RNA polymerase inhibitor and also stimulates the production of reactive oxygen species (*7, 8*). It exhibits a unique lasso-type structure that results from posttranslational cyclization of the Gly1 amino group and the side chain carboxylate of Glu8 (*9–12*). Posttranslational tailoring of the microcin C7 heptapeptide, produced by *E. coli* strains carrying the pMccC7 plasmid, forms a nonhydrolyzable phosphoramidate linkage between the peptide C-terminus and an aminopropyl-modified AMP moiety (*13–16*). Microcin C7 is a "Trojan horse" aspartyl tRNA synthetase inhibitor (*17*). The chromosomally encoded microcins E492m, H47, I47, and M are (or are predicted to be) ribosomal peptide−nonribosomal peptide conjugates where the NRPS product is attached to the ribosomal peptide C-terminus during maturation (*1, 18*).

Microcin E492m (MccE492m, Figure 1) is produced by *Klebsiella pneumoniae* RYC492 and displays a number of interesting structural features (*19–21*). The 84-residue ribosomal peptide portion contains a serine-rich C-terminus (SSSGYNSATSSSGSGS). Its C-terminal posttranslational modification consists of a linearized and C-glycosylated

[†] This work was supported by NIH Grant Al 47238 (C.T.W.) and an NIH postdoctoral fellowship (E.M.N.).

* Corresponding author: e-mail, christopher_walsh@hms.harvard.edu; phone, 617-432-1715; fax, 617-432-0438.

[1] Abbreviations: DHBS, *N*-(2,3-dihydroxybenzoyl)serine; Ent, enterobactin; MGE, monoglycosylated enterobactin; DGE, diglycosylated enterobactin; TGE, triglycosylated enterobactin; Glc-$DHBS_2$, glycosylated DHBS dimer; Glc-DHBS, glycosylated DHBS monomer; lin-MGE, linear MGE; TCEP, tris(2-carboxylethyl)phosphine; TFA, trifluoroacetic acid; NRPS, nonribosomal peptide synthetase; α-S-ATP, adenosine 5′-*O*-(1-thiophosphate); γ-S-ATP, adenosine 5′-*O*-(3-thiophosphate); App(NH)p, adenylyl imidodiphosphate; Mcc, microcin; MccE492, unmodified microcin E492; MccE492m, posttranslationally modified MccE492; FL, fluorescein; B, biotin; C_{10}, C-terminal decapeptide; RP, reverse phase; rt, room temperature.

10.1021/bi800826j CCC: $40.75
Published on Web 08/09/2008

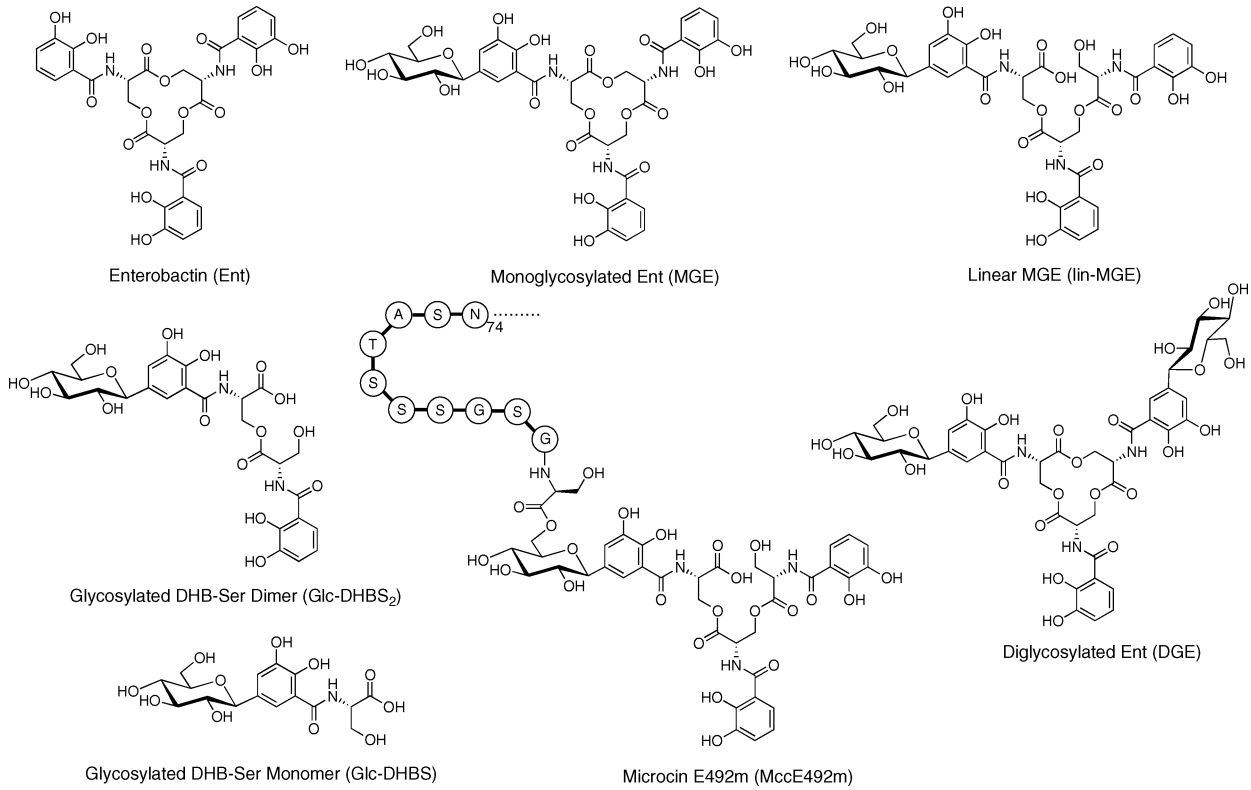

FIGURE 1: Structures of enterobactin, its glycosylated and hydrolyzed derivatives produced by the action of MceCD, and a truncated depiction of microcin E492m showing only the 11 C-terminal amino acids.

enterobactin derivative (lin-MGE, Figure 1) that is attached to the carboxyl moiety of Ser84 by an ester linkage (*21*). Enterobactin (Ent, Figure 1), an iron scavenger (siderophore) and virulence factor, is a cyclic trimer of *N*-(2,3-dihydroxybenzoyl)serine (DHBS) and is produced by NRPS machinery in Gram-negative bacteria during iron-deficient conditions (*22*). The lin-MGE moiety in MccE492m is structurally related to the salmochelins (*23*), C-glycosylated derivatives of enterobactin that exhibit improved hydrophilicity (*24*) and provide a means for enterobacteria to evade siderocalin, a protein component of the mammalian innate immune system (*25–27*). The glucose moiety in MccE492m is a bridging element that links the ribosomal and nonribosomal peptide fragments, both of which have distinct functional significance. The lin-MGE moiety affords MccE492m recognition by siderophore receptors (FepA, Cir, Fiu) on the cell surface/outer membrane of Gram-negative bacteria (*28, 29*). The antibiotic microcin peptide then causes pore formation, inner membrane depolarization, and cell death (*30, 31*). MccE492m is therefore a "Trojan horse" toxin that targets the iron uptake systems of enterobacteria. Recent work indicates that the mannose permease is required for MccE492m toxicity (*32*). Genetic predictions indicate that microcins H47, I47, and M, produced by various *E. coli* strains, also display serine-rich C-termini (*1, 18*). They presumably all display the same posttranslational modification, and share the same mechanism of action, as MccE492m.

The MccE492 gene cluster encodes 10 genes, *mceABCDEFGHIJ*, that orchestrate MccE492m production, export, and immunity (*33–36*). *mceA* encodes a 99- or 103-residue precursor peptide that undergoes cleavage at amino acid 15 or 19 prior to export. The *mceB* product is a 95-residue peptide required for producer immunity. *mceGH* are needed for toxin export, and the *mceE* gene product is also involved in export. The function of *mceF* is undefined. Four genes, *mceCDIJ*, are necessary and sufficient for MccE492m posttranslational maturation in a strain that produces enterobactin (*35, 37*). Overexpression, purification, and in vitro characterization of MceCDIJ provided a maturation pathway for MccE492m starting from MccE492 and enterobactin (*38*). MceC is a *C*-glycosyltransferase that attaches one or two glucose moieties to the C5 position(s) of the Ent scaffold. MceD is an enterobactin esterase that cleaves the macrolactone ring of Ent and its glycosylated congeners to afford linearized derivatives. The protein complex MceIJ is responsible for the posttranslational modification of MccE492. It attaches MGE/lin-MGE to the MccE492 C-terminus in an ATP- and Mg(II)-dependent manner (Scheme 1). Studies that employed the C-terminal decapeptide of MccE492 revealed that this reaction occurs at the C4′ glucose hydroxyl. Nonenzymatic and base-catalyzed migration of the glycosyl ester from C4′ to C6′ provides the connectivity observed in MccE492m isolated from bacterial cultures.

The MceIJ protein complex is interesting in several respects. It catalyzes a rare C-terminal posttranslational modification. Other examples of C-terminal posttranslational modifications include the installation of an adenosine moiety via a N−P bond in MccC7 (*16*) and the esterification of Ras (*39*). The mechanism of MccE492 C-terminal carboxylate activation by MceIJ is therefore of interest. Because MceIJ have few or no characterized homologues, the fate of the ATP cofactor and identities of critical residues are unclear. MccE492m analogues with Glc-$DHBS_2$ and Glc-DHBS moieties were identified in bacteria cultures recently (*37*). Determining if these siderophores are substrates for MceIJ is of biosynthetic relevance, and the peptide substrate scope of MceIJ is also worthy of consideration. The present work

Scheme 1: MceIJ-Catalyzed Attachment of MGE to the C-Terminal Serine Residue of C_{10}E492 via the C4′ Glucose Hydroxyl and Subsequent Base-Catalyzed Migration of the Glycosyl Ester to the C6′ Position

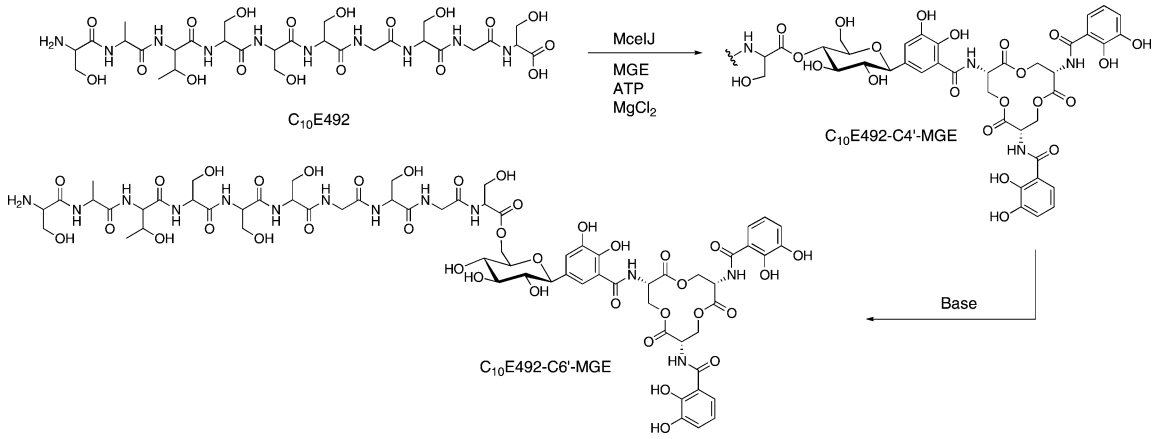

addresses the ATP utilization, mechanism, and substrate selectivity of MceIJ.

EXPERIMENTAL PROCEDURES

Materials and Methods. The nonhydrolyzable ATP analogues adenosine 5′-*O*-(3-thiophosphate) tetralithium salt (γ-S-ATP) and adenosine-5′-*O*-(1-thiophosphate) (α-S-ATP) were purchased from Alexis Biochemicals, and α- and β-*O*-phenylglycopyranoside were purchased from TCI America. All other chemicals were purchased from Sigma-Aldrich and used as received. Analytical and preparative HPLC were performed on a Beckman System Gold (Beckman Coulter) instrument. A Vydac (Hesperia, CA) C18 column (4.6 × 50 mm) at either 1 or 4 mL/min or a Vydac small-pore C18 column (34.6 × 250 mm) at 1 mL/min was employed for the activity assays and kinetic studies. In all cases, solvent A was 0.2% TFA/H_2O and solvent B was 0.2% TFA/MeCN. A Vydac 302IC4.610 (4.6 × 100 mm) column at 2 mL/min was employed for analytical ion-exchange chromatography with a solvent gradient of 0% B for 2 min followed by 1−100% B in 17 min (solvent A, 25 mM total 1:1 NaH_2PO_4/Na_2HPO_4 at pH 2.8; solvent B, 125 mM total 1:1 NaH_2PO_4/Na_2HPO_4 at pH 2.9). Absorption was generally monitored at 220 and 316 nm. The latter wavelength corresponds to enterobactin catecholate absorption. For the ATP utilization assays, adenosine absorption (260 nm) was monitored to detect AMP, ADP, and ATP by RP-HPLC and ion-exchange chromotagraphy. A Shimadzu LCMS-QP800a outfitted with a Higgins Analytical (Mountainview, CA) Sprite Targa C18 column (2.1 × 20 mm) was employed for LCMS.

Wild-Type MceIJ and Substrate Preparations. MceIJ was overexpressed in *E. coli* and purified as previously described (*38*). The siderophore substrates monoglycosylated enterobactin (MGE), linearized monoglycosylated enterobactin (lin-MGE), the glycosylated DHB-Ser dimer (Glc-$DHBS_2$), glycosylated DHB-Ser monomer (Glc-DHBS), and diglycosylated enterobactin (DGE) were prepared by MceC- and MceD-catalyzed modifications of enterobactin (Ent) as described elsewhere (*38*). The ferric complexes of MGE and DGE, $[Fe(MGE)]^{3-}$ and $[Fe(DGE)]^{3-}$, were synthesized from ferric chloride and the siderophore of choice as previously reported (*38*). The preparation of 6-deoxyMGE is provided as Supporting Information. Stock solutions of siderophores were prepared in DMSO or Millipore water, divided into aliquots, and stored at −20 °C. The stock solution concentrations (∼4 to ∼12 mM) were verified using the reported (*40*) extinction coefficients for enterobactin (316 nm, 9500 M^{-1} cm^{-1}), linear enterobactin (315 nm, 9700 M^{-1} cm^{-1}), and $[Fe(Ent)]^{3-}$ (338 nm, 15100 M^{-1} cm^{-1}), with the assumption that any glucose moieties have no effect on siderophore absorption. For Glc-$DHBS_2$ and Glc-DHBS, the contribution of two and one catechols to lin-Ent absorption at 315 nm was considered. All peptides were synthesized by standard Fmoc solid-phase peptide synthesis at the Biopolymers Facility at Harvard Medical School, and their sequences are provided in Table 1. Their purities and identities were confirmed by analytical HPLC and LCMS. In some instances, the peptides were further purified by preparative HPLC. The N-terminally modified peptides FL-C_{10}E492 and B-C_{10}E492 were further purified by preparative HPLC using a gradient of 0−40% B in 40 min. With the exception of B-C_{10}E492, all peptide stock solutions (∼2 to ∼12 mM) were prepared in Millipore water, and their concentrations were verified by quantitative amino acid analysis (Dana Farber Cancer Institute, Boston, MA). The B-C_{10}E492 peptide stock solution (2.0 mM) was prepared in spectrophotometric grade DMSO. The peptide stock solutions were partitioned into aliquots and stored at −20 °C.

Table 1: Peptide Names and Sequences

name	sequence
C_7E492	SSSGSGS
C_{10}E492	SATSSSGSGS
C_{13}E492	GYNSATSSSGSGS
C_{15}E492	SSGYNSATSSSGSGS
C_{10}E492(S10G)	SATSSSGSGG
C_{10}E492(S10A)	SATSSSGSGA
C_{10}E492(S10T)	SATSSSGSGT
C_{10}H47	SASSSAGGGS
C_{10}I47	SSTSSAVSGS
C_{10}M	SASSSAGSGS
FL-C_{10}E492	fluorescein-SATSSSGSGS
B-C_{10}E492	biotin-SATSSSGSGS

Site-Directed Mutagenesis of MceI. A Quick-Change site-directed mutagenesis protocol (Stratagene) was used to generate the C29A, C109A, C110A, H5A, H54A, H93A, and H151A mutations in *mceI* using pET-28b-mceIJ as a template and Pfu Turbo DNA polymerase (Stratagene). This template provides a N-terminal His_6 tag on MceJ and no tag on MceI (*38*). The primers and primer pairings employed are listed in Table S1 (Supporting Information). Following

PCR amplification, the residual template plasmid was digested with *Dpn*I (2 μL added to a 50 μL PCR reaction) for 3 h at 37 °C. The PCR products were transformed into *E. coli* TOP10 cells (Stratagene) and the purified plasmids obtained using a Miniprep kit (Qiagen). The DNA sequences and presence of the desired mutations were verified by DNA sequencing (Dana Farber Cancer Institute, Boston, MA). Expression constructs were transformed into *E. coli* BL21(DE3) cells (Stratagene). Overexpression and purification of the mutants were conducted as described previously for wild-type MceIJ (*38*). In each case, a MceIJ protein complex was isolated following Ni-NTA affinity chromatography.

The SOE mutagenesis approach (*41*) was employed to generate the H32A mutant in *mceI* using the primers and primer pairings listed in Table S1 and pET-28b-MceIJ as a template. The products from the two rounds of PCR amplification were digested with *Xho*I and *Nde*I (New England Biolabs), ligated into the pET-28b expression vector using T4 DNA ligase (New England Biolabs), and transformed into *E. coli* TOP10 cells. The identity of the resulting pET28b-mceI(H32A)J construct was verified by DNA sequencing, and it was transformed into *E. coli* BL21(DE3) cells. Overexpression and purification of MceI(H32A)J were performed as previously described for the wild-type protein complex (*38*).

Initial Velocity Assays with MceIJ. All initial velocity assays were conducted in buffer A (75 mM Tris-HCl, pH 8, 5 mM $MgCl_2$, 2.5 mM TCEP). The assays were generally conducted with 2 μM MceIJ and substrate concentrations of 100 and 500 μM for the siderophore and peptide, respectively. A 5 mM concentration of ATP was used in preliminary studies. Subsequent work indicated that the MceIJ-catalyzed modification of C_{10}E492 with MGE was inhibited at [ATP] > 1 mM (data not shown), and all subsequent assays were therefore carried out in the presence of 500 μM ATP. Reaction aliquots were quenched by addition of an equal volume of 0.6% TFA/H_2O. The quenched mixtures were vortexed, centrifuged (13000 rpm × 10 min), stored on ice or at −20 °C, and analyzed by analytical RP-HPLC. The solvent gradients employed were (i) 0−40% B for all assays with MGE, $[Fe(MGE)]^{3-}$, DGE, or $[Fe(DGE)]^{3-}$ as the siderophore substrate, (ii) 0−30% B for assays with Glc-$DHBS_2$, and (iii) 0−20% B for assays with Glc-DHBS. To determine product identity, the product peaks were collected following elution from the analytical HPLC column and lyophilized, and the residues were redissolved in 25−100 μL of Millipore water and analyzed by LCMS. Assays that employed nonhydrolyzable ATP analogues or alternative sugars were performed analogously using a solvent gradient of 0−40% B for HPLC analysis.

Identification of AMP as a Reaction Product. Reactions in buffer A that contained 500 μM C_{10}E492, 100 μM MGE, 2 μM MceIJ, and 500 μM ATP or lacked one or more components were quenched with an equal volume of 0.6% TFA/H_2O at t = 20 min, vortexed, centrifuged (13000 rpm × 10 min), and analyzed by RP-HPLC or ion-exchange chromatography using UV detection at 220 and 260 nm. The traces were compared to those of authentic ATP, ADP, and AMP standards. A gradient of 0−40% B in 8 min was employed for RP-HPLC, which gave a retention time of ~0.8 min for AMP. Ion-exchange chromatography employing a phosphate buffering system (see above) provided separation of AMP, ADP, and ATP with retention times of 1.8, 8, and 16.5 min, respectively. The identity of the AMP product peak was confirmed by MS: calcd $[M - H]^-$, 346.0; found, 346.1.

ATP-PP_i Exchange Assay. Reactions were prepared in buffer A containing MceIJ (2 μM), ATP (500 μM or 1 mM), sodium [^{32}P]pyrophosphate (800000 cpm), and either MGE (100 μM) or C_{10}E492 (500 μM). The 500 μL reactions were incubated at room temperature, and 100 μL aliquots were quenched at time points ranging from 0 to 240 min with 500 μL of an aqueous solution containing 1.6% (w/v) activated charcoal, 200 mM tetrasodium phyrophosphate, and 3.5% perchloric acid. The charcoal was pelleted by ultracentrifugation (13000 rpm × 10 min) and washed (2 × 500 μL) with an aqueous solution containing 200 mM tetrasodium pyrophosphate and 3.5% perchloric acid. The radioactivity bound to the charcoal was subsequently measured by liquid scintillation counting.

Kinetic Investigations of MceIJ. All kinetic studies designed to determine the apparent k_{cat} and K_M values for the decapeptide substrates were carried out in buffer A with 500 μM ATP and 100 μM MGE. The peptide concentrations were varied from 10 μM to 1.5 mM. The MceIJ concentrations and time points were chosen such that only formation of the C4′ glycosyl ester product was observed. The MceIJ concentrations employed were 1 (C_{10}E492, FL-C_{10}E492, C_{10}M, C_{10}I47), 2 (C_{10}H47, C_{10}S10A), or 4 (C_{10}S10T) μM. With the exception of the FL-C_{10}E492 reactions, which were each 50 μL, the reaction volumes were 100 μL. The reactions were quenched by addition of an equal volume of 0.6% TFA/H_2O at t = 3 (C_{10}I47), 4 (FL-C_{10}E492), or 5 (C_{10}E492, C_{10}M, C_{10}H47, C_{10}S10A, C_{10}S10T) min, vortexed, centrifuged (13000 rpm × 10 min), stored on ice, and analyzed by HPLC using a solvent gradient of 0−40% B. A Vydac C18 column (4.6 × 50 mm) at 4 mL/min was employed for the C_{10}E492, FL-C_{10}E492, C_{10}I47, C_{10}H47, and C_{10}M samples. A Vydac small-pore C18 column (94.6 × 250 mm) at 1 mL/min was employed for the C_{10}S10A and C_{10}S10T samples. With the exception of FL-C_{10}E492, product quantification was based on the area of the 316 nm absorption peaks. Because both MGE and FL-C_{10}E492 absorb at 316 nm, product quantification for FL-C_{10}E492-MGE was based on maximum fluorescein absorption (440 nm in either 0.2% TFA/H_2O or 0.2% TFA/MeCN). With the exception of FL-C_{10}E492, which was repeated only in duplicate because of a limited quantity of substrate, all kinetic runs were repeated in triplicate. The data were fit to the Michaelis−Menten equation.

RESULTS

ATP Utilization by MceIJ. To determine the fate of the ATP during the MceIJ-catalyzed modification of C_{10}E492 with MGE (Scheme 1), we first utilized nonhydrolyzable ATP analogues as cofactors (Figure 2). No product formation was observed when α,β- or β,γ-methylene ATP were employed; these ATP analogues inhibited MceIJ (data not shown). Substitution of ATP with App(NH)p or γ-S-ATP resulted in C_{10}E492-MGE formation whereas no products were observed with α-S-ATP. These results indicated attack at P_α and cleavage of the high-energy α,β bond of ATP during the MceIJ-catalyzed reaction.

AMP was subsequently identified as a reaction product by HPLC, ion-exchange chromatography, and mass spec-

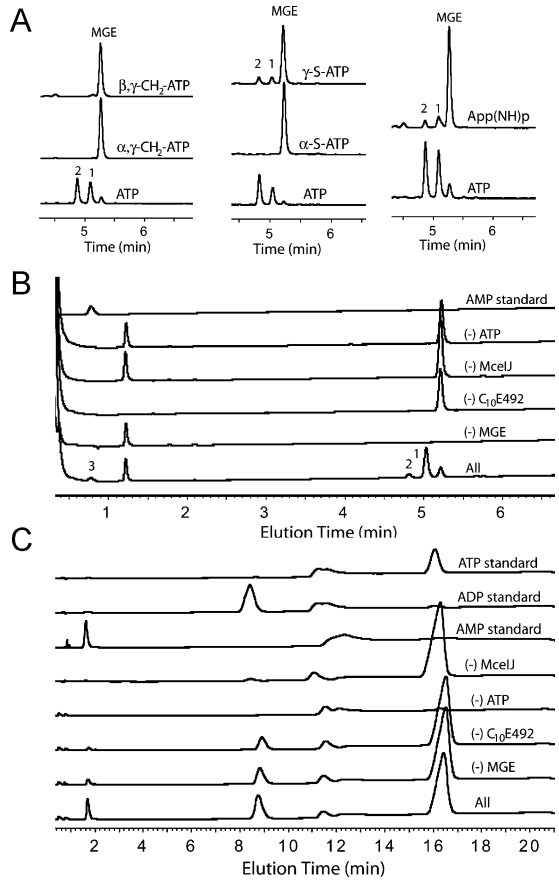

FIGURE 2: ATP utilization by MceIJ. (A) HPLC traces for 3 h incubations conducted at room temperature in buffer A with MceIJ, C_{10}E492, MGE, and either ATP or a nonhydrolyzable ATP analogue (316 nm detection). Left: No product formation observed with α,β- or β,γ-methylene ATP (α,β-CH_2-ATP and β,γ-CH_2-ATP, respectively). Middle: Product formation occurs with γ-S-ATP but not α-S-ATP. Right: Product formation is observed with App(NH)p. (B) Detection of AMP by RP-HPLC (220 nm detection). (C) Detection of AMP by ion-exchange chromatography (260 nm detection). Background hydrolysis of ATP to ADP and P_i is observed in the presence of enzyme. Peak numbers 1 and 2 refer to C_{10}E492-C4′-MGE and C_{10}E492-C6′-MGE, respectively. The corresponding *m*/*z* values are provided in Table 2.

trometry (Figure 2). The HPLC traces revealed formation of a new peak with 260 nm absorption, characteristic of an adenosine moiety, that coeluted with an authentic AMP standard (retention time ~ 0.8 min) following incubation of MceIJ with C_{10}E492, MGE, and ATP in buffer A. No product was observed in reactions that lacked one or more of the components. Isolation of the ~0.8 min peak and subsequent MS analysis provided a *m*/*z* value consistent with AMP ([M − H]$^-$, calcd, 346.1; found, 346.0). Analysis of the reaction mixtures by ion-exchange chromatography, which provided clear separation of AMP, ADP, and ATP, revealed background ATP hydrolysis by the MceIJ protein preparation. The origins of the basal ATP hydrolysis to ADP and P_i were not pursued. No ATP−PP_i exchange was observed following incubation of MceIJ with Mg(II), ATP, [^{32}P]pyrophosphate, and either C_{10}E492 or MGE (data not shown).

Site-Directed Mutagenesis of MceI. Site-directed mutagenesis was employed to determine if any of the three Cys or five His residues in MceI are required for catalysis. The mutant proteins were overexpressed in *E. coli* BL21(DE3) cells and purified by nickel affinity chromatography using a step gradient of increasing concentrations of imidazole. The

Table 2: *m*/*z* Data for MceIJ Reaction Products[a]

peak	identity	calcd *m*/*z*	found *m*/*z*
1	C_{10}E492-C4′-MGE	[M + H]$^+$, 1640.6	1640.2
2	C_{10}E492-C6′-MGE	[M + H]$^+$, 1640.6	1640.2
3	AMP	[M − H]$^-$, 346.1	346.0
4	C_{10}E492-C4′-(6-deoxyMGE)	[M − 2H]$^{2-}$/2, 810.8	810.8
5	C_{10}E492-(6-deoxyMGE)	[M − 2H]$^{2-}$/2, 810.8	810.8
	C_{10}E492-C4′-(lin-MGE)	[M + H]$^+$, 1658.6	1658.0
	C_{10}E492-C6′-(lin-MGE)	[M + H]$^+$, 1658.6	1658.1
	C_{10}E492-(lin-MGE)	[M + H]$^+$, 1658.6	1658.1
6	C_{10}E492-C4′-(Glc-$DHBS_2$)	[M + H]$^+$, 1435.5	1435.3
7	C_{10}E492-C6′-(Glc-$DHBS_2$)	[M + H]$^+$, 1435.5	1435.3
8	C_{10}E492-(Glc-$DHBS_2$)	[M + H]$^+$, 1435.5	1435.4
9	C_{10}E492-C4′-(Glc-DHBS)	[M + H]$^+$, 1212.4	1212.2
10	C_{10}E492-C6′-(Glc-DHBS)	[M + H]$^+$, 1212.4	1212.2
11	C_{10}E492-(Glc-DHBS)	[M + H]$^+$, 1212.4	1212.3
12	C_{10}E492-(Glc-DHBS)	[M + H]$^+$, 1212.4	1212.4
13	C_{10}E492-C4′-DGE	[M − 2H]$^{2-}$/2, 899.8	899.8
14	C_{10}E492-C6′-DGE	[M + H]$^+$, 1802.6	1802.6
	C_{10}E492-C4′-MGE[b]	[M − H]$^-$, 1638.5	1638.5
	C_{10}E492-C6′-MGE[b]	[M + H]$^+$, 1640.6	1640.6
	C_{10}E492-C4′-DGE[b]	[M + 2H]/2, 901.8	901.5
	C_{10}E492-C6′-DGE[b]	[M + 2H]/2, 901.8	902.0
15	C_7E492-C4′-MGE	[M + H]$^+$, 1381.4	1381.1
16	C_7E492-C6′-MGE	[M + H]$^+$, 1381.4	1381.2
	C_{13}E492-C4′-MGE	[M + 2H]$^{2+}$, 987.8	987.8
17	C_{10}H47-C4′-MGE	[M + H]$^+$, 1580.5	1580.9
18	C_{10}H47-C6′-MGE	[M + H]$^+$, 1580.5	1580.8
19	C_{10}I47-C4′-MGE	[M + 2H]$^{2+}$/2, 849.3	849.6
20	C_{10}I47-C6′-MGE	[M + H]$^+$, 1697.5	1697.8
21	C_{10}M-C4′-MGE	[M + H]$^+$, 1610.5	1610.9
22	C_{10}M-C6′-MGE	[M + H]$^+$, 1610.5	1610.5
23	C_{10}E492(S10A)-C4′-MGE	[M + H]$^+$, 1624.5	1624.8
24	C_{10}E492(S10A)-C6′-MGE	[M + H]$^+$, 1624.5	1624.9
25	C_{10}E492(S10T)-C4′-MGE	[M + 2H]$^{2+}$/2, 827.8	827.7
26	C_{10}E492(S10T)-C6′-MGE	[M + 2H]$^{2+}$/2, 827.8	827.7
27	B-C_{10}E492-C4′-MGE	[M + 2H]$^{2+}$/2, 933.8	933.8
28	B-C_{10}E492-C6′-MGE	[M + 2H]$^{2+}$/2, 933.8	933.7
29	FL-C_{10}E492-C4′-MGE	[M + 2H]$^{2+}$/2, 999.8	1000.1
30	FL-C_{10}E492-C6′-MGE	[M + 2H]$^{2+}$/2, 999.8	999.8

[a] The C_{10}E492-MGE and C_{10}E492-(lin-MGE) data were taken from ref *38*. [b] For assays conducted using [Fe(MGE)]$^{3-}$ or [Fe(DGE)]$^{3-}$ as substrates.

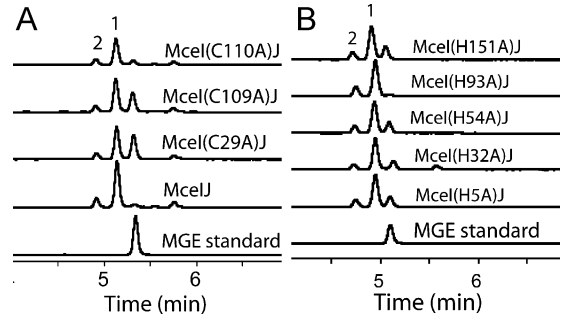

FIGURE 3: Activity of the Cys (panel A) and His (panel B) mutants. HPLC traces (316 nm) of reactions in buffer A containing 4 μM enzyme, 100 μM MGE, 500 μM C_{10}E492, and 500 μM ATP (rt, t = 30 min). Peak numbers 1 and 2 refer to C_{10}E492-C4′-MGE and C_{10}E492-C6′-MGE, respectively. The corresponding *m*/*z* values are provided in Table 2.

mutants exhibited nickel affinity comparable to the wild type. Analysis by SDS−PAGE revealed that each mutant was isolated as a MceIJ protein complex (Figure S1).

The eight mutants all displayed activity in HPLC assays following incubation with MGE, C_{10}E492, and ATP (Figure 3). These observations indicate that there is no acyl-S-MceI intermediate in the MceIJ catalytic cycle and that there is no structurally or catalytically required His residue in MceI.

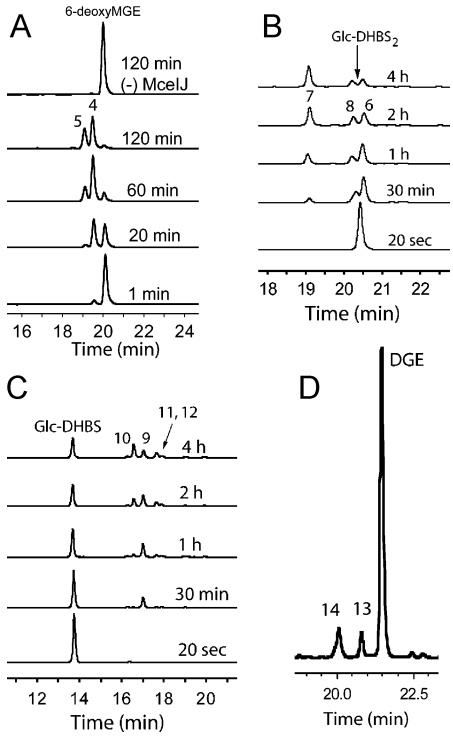

FIGURE 4: Activity assays monitored by HPLC with 316 nm detection for the MceIJ-catalyzed attachment of various glycosylated siderophores to the C_{10}E492 C-terminus. (A) Activity assay with 6-deoxyMGE. (B) Activity assay with Glc-$DHBS_2$. (C) Activity assay with Glc-DHBS. (D) A single trace from an activity assay with DGE ($t = 2$ h). The corresponding *m*/*z* data are provided in Table 2.

6-DeoxyMGE Is a Substrate of MceIJ. MceIJ attaches MGE to C_{10}E492 via the C4′ hydroxyl, and subsequent migration to the C6′ position affords the mature MccE492m connectivity. To further validate initial attack by the glucosyl C4′ hydroxyl, we evaluated 6-deoxyMGE as a substrate for MceIJ (Figure 4). The synthesis of 6-deoxyMGE required UDP-6-deoxyglucose, which was prepared chemoenzymatically (Scheme S1). 6-Deoxyglucose-1-phosphate was first synthesized in three steps from 6-deoxyglucose. RmlA, the glucose-1-phosphate thymidylyl transferase from *Salmonella enterica* serovar *Typhimirium* LT2 that recognizes and modifies a variety of natural and synthetic sugars to provide the TDP and UDP analogues (*42*), was cloned from *Salmonella enterica* serovar *Typhimirium* LT2 genomic DNA (*43*) (Supporting Information). It was overexpressed in *E. coli* BL21(DE3) cells as a N- or C-terminal His_6 fusion, purified by nickel affinity chromatography, and obtained in yields of >30 mg/L (Figure S2). Addition of IroB (*44*), the *C*-glycosyltransferase from the *iroA* gene cluster, and Ent to reactions containing RmlA, UTP, Mg(II), and 6-deoxyglucose 1-phosphate, which generated UDP-6-deoxyglucose in situ, provided mixtures of Ent, 6-deoxyMGE, 6-deoxyDGE, and 6-deoxyTGE, which were separated by preparative HPLC and analyzed by MS (Figure S3). Incubation of 6-deoxyMGE with MceIJ, C_{10}E492, and ATP in buffer A for 1 min resulted in formation of a new peak in the analytical HPLC trace with 316 nm absorption and a *m*/*z* value consistent with attachment of 6-deoxyMGE to the C_{10}E492 peptide via an ester linkage (calcd $[M - 2H]^{2-}/2$, 810.8; found, 810.8) (Figure 4). At longer time points, a second peak with catecholate absorption, a shorter retention time, and a *m*/*z* value also consistent with C_{10}E492-(6-deoxyMGE) formed. We presume that MceIJ attaches C_{10}E492 to the C4′ position of 6-deoxyMGE and that the second peak corresponds to an unexpected structural isomer. Qualitative comparisons suggest that the glycosyl ester migration rate in C_{10}E492-C4′-(6-deoxyMGE) is slower than that of C_{10}E492-C4′-MGE.

Siderophore Selectivity of MceIJ. Assays were conducted to determine if MceIJ accepts and links Glc-$DHBS_2$, Glc-DHBS, and DGE, produced by MceC and MceD, to C_{10}E492 (Table 2, Figure 4). Incubation of MceIJ in buffer A with C_{10}E492, Glc-$DHBS_2$, and ATP resulted in the formation of three new peaks in the analytical HPLC trace with *m*/*z* values consistent with [C_{10}E492 + Glc-$DHBS_2$ − H_2O] and attachment of Glc-$DHBS_2$ to the decapeptide C-terminus via an ester linkage that then rearranges by acyl migrations. Glc-DHBS was also accepted by MceIJ and transferred to C_{10}E492. Four new peaks were observed in the analytical HPLC trace with *m*/*z* values consistent with formation of C_{10}E492-(Glc-DHBS). A comparison of the time courses for Glc-$DHBS_2$ and Glc-DHBS with that of MGE as the nucleophilic substrate indicates that the relative rate of C_{10} modification by MceIJ with Glc-DHBS is lower than that of MGE or Glc-$DHBS_2$.

Because monomeric Glc-DHBS was accepted, we evaluated other glycosides with substitution at C1′ as substrates for MceIJ (data not shown). Activity assays indicated that α- and *β*-*O*-phenylglycopyranoside are neither substrates nor inhibitors of MceIJ. Carminic acid, which has an anthraquinone derivative linked to glucose by a C−C bond at the C1′ position, did inhibit MceIJ.

Incubation of MceIJ with C_{10}E492, DGE, and ATP in buffer A resulted in the formation of two new peaks in the analytical HPLC trace consistent with C4′ and C6′ glycosyl ester formation and with *m*/*z* values equal to C_{10}E492-DGE (Table 2, Figure 4). Less formation of C_{10}E492-DGE (∼23%) was observed than for C_{10}E492-MGE (∼80%) under identical reaction conditions (100 μM siderophore, 500 μM C_{10}E492, 5 mM ATP, $t = 3$ h). No evidence for a DGE-based product with two linked peptides, one to each glucose moiety, was observed.

Ent and its glycosylated congeners are iron chelators. We therefore investigated if MceIJ recognizes $[Fe(MGE)]^{3-}$ and $[Fe(DGE)]^{3-}$ as substrates. Incubation of MceIJ with $[Fe(MGE)]^{3-}$, C_{10}E492, and ATP in buffer A resulted in a product distribution that mirrors that of MGE (Figure S4). LCMS analysis of the product peak with 316 nm absorption revealed *m*/*z* values consistent with formation of a glycosyl ester linkage between C_{10}E492 and $[Fe(MGE)]^{3-}$ (Table 2). Likewise, incubation of $[Fe(DGE)]^{3-}$ with C_{10}E492 and ATP resulted in a product distribution and rate of reaction similar to those of DGE (data not shown).

Kinetic studies were initiated to ascertain the preference of MceIJ for a given siderophore substrate. Preliminary studies indicated that the apparent K_M values of MceIJ for MGE and $[Fe(MGE)]^{3-}$ were too low (<3 μM) for reliable quantification by the HPLC assay. As a result, no further kinetic characterization for the siderophore substrate K_M values were conducted.

Peptide Selectivity of MceIJ. Our initial evaluation of MceIJ activity was based on a model system comprised of MGE and the C-terminal decapeptide (SATSSSGSGS)

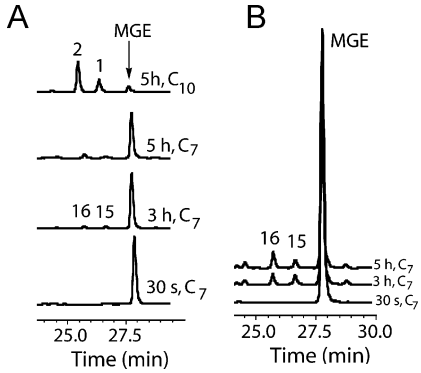

FIGURE 5: HPLC assay of MceIJ with C_7E492 as the peptide substrate. (A) Time course of the MceIJ-catalyzed reaction in buffer A with 500 μM C_7E492, 100 μM MGE, and 5 mM ATP. The top trace is of a reaction where C_{10}E492 was employed for comparison. (B) Expansion of the traces for C_7E492-MGE formation to exemplify the C4′ to C6′ migration.

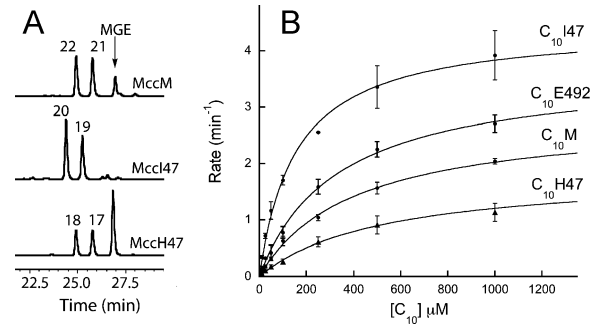

FIGURE 6: The C-terminal decapeptides of microcins H47, I47, and M are substrates for MceIJ. (A) Initial activity assays. HPLC traces (316 nm detection) of MceIJ-catalyzed reactions in buffer A containing 2 μM enzyme, 100 μM MGE, 500 μM decapeptide, and 5 mM ATP (rt, $t = 2.5$ h). Table 2 lists the corresponding *m*/*z* data. (B) Kinetic traces for the MceIJ-catalyzed linkage of MGE and C_{10}E492, C_{10}H47, C_{10}I47, and C_{10}M. The corresponding kinetic parameters are listed in Table 3.

of the 84-residue MccE492 (Scheme 1) (*38*). With the aims of optimizing the model system and determining the minimal requirement for peptide recognition by MceIJ, the C-terminal peptides C_7E492, C_{13}E492, and C_{15}E492 were considered (Table 1). Initial activity assays indicated that MceIJ accepted each peptide and that two product peaks with 316 nm absorption formed, consistent with initial formation of the C4′ glycosyl ester and subsequent migration to the C6′ position. A comparison of the HPLC traces for the reaction mixtures indicated that MceIJ processed the C_{10}, C_{13}, and C_{15} peptides with similar relative rates (data not shown). In contrast, C_7E492 was not a good substrate for MceIJ (Figure 5). Only ~8% product formation was observed with C_7E492 compared to ~80% with C_{10}E492 following a 3 h incubation of MceIJ with 100 μM MGE, 500 μM peptide, and 5 mM ATP. Lowering the ATP concentration to 500 μM had negligible effect on the rate of C_7E492 modification by MceIJ. All subsequent assays were therefore conducted with decapeptide model substrates.

Microcins H47, I47 and M, produced by *E. coli* strains, are structurally related to MccE492m from *Klebsiella* (*18*). We therefore evaluated if MceIJ recognizes and modifies the C-termini of MccH47, MccI47, and MccM using C-terminal decapeptides as model substrates. Initial activity assays with MceIJ, MGE, ATP, and C_{10}H47/I47/M revealed that the C-terminal decapeptides of microcins H47, I47, and M are all substrates for MceIJ. In each case, two new product peaks with 316 nm absorption were observed in the analytical HPLC trace with masses consistent with C_{10}-MGE formation and linkage through a glycosyl ester (Table 2, Figure 6). Kinetic characterization was conducted to determine the apparent k_{cat} and K_M values for each decapeptide substrate (Table 3, Figure 6). The apparent k_{cat} values range from 1.84 $\pm$ 0.1 min^{-1} (C_{10}H47) to 4.44 $\pm$ 0.15 min^{-1} (C_{10}I47), and the apparent K_M values vary from 158 $\pm$ 16 μM (C_{10}I47) to 528 $\pm$ 67 μM (C_{10}H47). These values indicate that MceIJ has little preference for a given decapeptide.

To determine if the C-terminal serine hydroxyl moiety of MccE492/H47/I47/M is required for MceIJ-catalyzed modification of the decapeptide, we evaluated C_{10}E492(S10G) and C_{10}E492(S10A) as substrates for MceIJ (Figure 7). Initial activity assays indicated that C_{10}E492(S10G) is not a substrate. C_{10}E492 was modified with MGE when a 1:1 ratio of C_{10}E492 and C_{10}E492(S10G) was employed, which indicated that C_{10}E492(S10G) is not an effective inhibitor (data not shown). In contrast, C_{10}E492(S10A) was accepted by MceIJ, and two new peaks with 316 nm absorption formed in the analytical HPLC trace, consistent with initial attachment of the decapeptide to the C4′ glucose hydroxyl and subsequent migration of the glycosyl ester to the C6′ position (Table 2, Figure 7). Kinetic analysis provided apparent k_{cat} and K_M values of 2.81 $\pm$ 0.17 min^{-1} and 256 $\pm$ 41 μM, respectively, and a catalytic efficiency comparable to that of C_{10}E492 (Table 3). C_{10}E492(S10T) was subsequently considered. It was accepted by MceIJ, but with a ~10-fold lower catalytic efficiency relative to C_{10}E492 (Table 3, Figure 7), which suggests that the extra methyl group of the Thr side chain may be a steric deterrent.

We hypothesized that MceIJ might accept decapeptides with modified N-termini. Initial activity assays employing C_{10}E492 analogues with either fluorescein (FL-C_{10}E492) or biotin (B-C_{10}E492) moieties linked to the decapeptide N-terminus and MGE provided FL-C_{10}E492-MGE and B-C_{10}E492-MGE conjugates. In both cases, the formation of two new peaks with 316 nm absorption was observed in the analytical HPLC trace consistent with formation of C4′ and C6′ glycosyl esters (Table 2, Figure 8). A comparison of the time courses for attachment of MGE to C_{10}E492, B-C_{10}E492 and FL-C_{10}E492 suggested similar processing. Kinetic evaluation of FL-C_{10}E492 revealed a catalytic efficiency of 16 $\times$ 10^{-3} μM^{-1} min^{-1} (Table 3, Figure S5), which is within 2-fold of the native C_{10}E492 peptide. Because of the poor solubility of B-C_{10}E492 in aqueous solution and the millimolar decapeptide concentrations required for kinetic characterization, its apparent k_{cat} and K_M values were not determined.

DISCUSSION

Microcins are structurally and functionally diverse antibiotic peptides. Many microcins display unique posttranslational modifications that are essential for physiological function and interaction with specific targets in susceptible bacterial cells (*1*). The four tailoring enzymes of the MccE492 gene cluster, MceCDIJ, provide a rare example of a posttranslational modification that occurs at a C-terminus and links ribosomal and nonribosomal peptides. Our initial report on the MceIJ protein complex revealed that it has

Table 3: Kinetic Parameters for MceIJ[a]

	C_{10}E492	C_{10}E492(S10A)	C_{10}E492(S10T)	C_{10}M	C_{10}H47	C_{10}I47	FL-C_{10}E492
k_{cat} (min^{-1})	3.66 ± 0.15	2.81 ± 0.17	0.78 ± 0.05	2.84 ± 0.10	1.84 ± 0.10	4.44 ± 0.15	1.17 ± 0.07
K_M (μM)	335 ± 33	256 ± 41	818 ± 11	404 ± 38	528 ± 67	158 ± 16	73 ± 16
k_{cat}/K_M (min^{-1} μM^{-1})	11 × 10^{-3}	11 × 10^{-3}	0.95 × 10^{-3}	7 × 10^{-3}	3.5 × 10^{-3}	30 × 10^{-3}	16 × 10^{-3}

[a] Experiments were conducted at room temperature in buffer A with 500 μM ATP and 100 μM MGE.

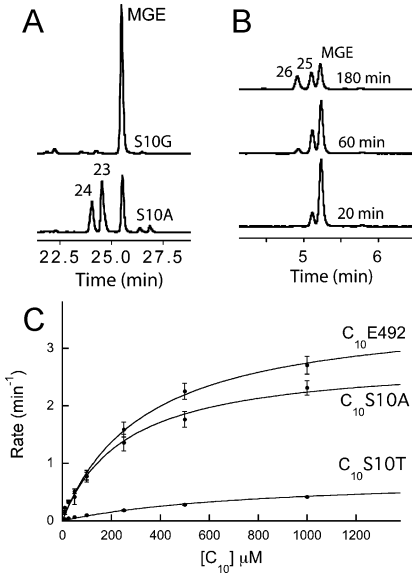

FIGURE 7: Analysis of decapeptide substrates with mutated C-terminal residues. (A) HPLC traces of incubations in buffer A with 2 μM MceIJ, 100 μM MGE, 5 mM ATP, and either 500 μM C_{10}E492(S10A) or 500 μM C_{10}E492(S10G) (rt, $t = 3$ h). No product formation for C_{10}E492(S10G) occurs whereas formation of C4′- and C6′-linked C_{10}E492(S10A)-MGE is observed. The corresponding *m/z* values are provided in Table 2. (B) Time course for the attachment of MGE to the C_{10}E492(S10T) C-terminus. The reactions were prepared as described for (A). (C) Kinetic traces for the MceIJ-catalyzed modification of C_{10}E492, C_{10}E492(S10A), and C_{10}E492(S10T) with MGE. The corresponding k_{cat} and K_M values are listed in Table 3.

ligase activity; it joins MccE492 and MGE/lin-MGE in an ATP-dependent reaction (*38*). MceIJ have few known homologues, and bioinformatic analysis therefore provides few clues about the MceIJ mechanism. MceI shares weak homology with HlyC, the acyltransferase responsible for hemolysin toxin activation (*45*). It also has an uncharacterized homologue, MchD, from the microcin H47 gene cluster (*46, 47*). MceJ has no known homologues other than its microcin H47 gene cluster counterpart MchC, which is also uncharacterized.

Based on our in vitro studies, we propose a mechanism for the MceIJ-catalyzed linkage of C_{10}E492 and MGE (Scheme 2) that requires formation and breakdown of a peptidyl-CO-AMP intermediate. The α-carboxylate of the C_{10}E492 C-terminal serine residue first attacks P_α of ATP, affording the peptidyl-CO-AMP intermediate. The first step of the MceIJ reaction resembles those of E1 family members (*48, 49*), which are involved in ubiquitin activation, and ThiF (*50, 51*) from thiamin biosynthesis; these enzymes have proteins as substrates, and they activate the protein C-terminal carboxylate as a peptidyl-CO-AMP. The ATP cleavage pattern of MceIJ is also similar to the first step of the MccB-catalyzed attachment of AMP to the MccC7 heptapeptide C-terminus (*16*). In another parallel, carboxyl activation of free amino acids by adenylyl transfer is the

Scheme 2: Mechanism for the MceIJ-Catalyzed Modification of the C_{10}E492 C-Terminus

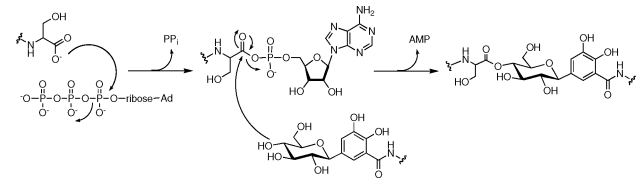

mechanism of aminoacyl-tRNA synthetases; the activated aminoacyl-AMP intermediates are captured by specific tRNA cosubstrates (*52*). Because peptide-dependent ATP/PP_i exchange was not observed for MceIJ, the C_{10}E492-CO-AMP is either tightly bound to MceIJ or its formation is not readily reversible.

The C4′ hydroxyl of MGE subsequently attacks the peptidyl-CO-AMP carbonyl moiety, which results in formation of a tetrahedral adduct, subsequent expulsion of AMP, and C4′ glycosyl ester formation. This step is similar to the nucleophilic attack of a C-terminal aminoacyl-AMP by the 3′-OH of ribose in aminoacyl tRNA formation, which results in oxoester products, and contrasts the capture of the peptidyl-CO-AMP intermediates in ubiquitin activation and thiamin biosynthesis. In ubiquitin activation, a Cys thiolate residue in E1 attacks the ubiquitnyl-CO-AMP intermediate formed by E1 to generate a thioester (*48*). In thiamin biosynthesis, the adenylated ThiS-CO-AMP intermediate formed by ThiF is converted to the ThiS-ThiF acyl disulfide, which is the sulfur donor for thiazole ring formation (*50, 51, 53, 54*).

Nonenzymatic and base-catalyzed migration of the C4′ glycosyl ester to the C6′ position affords the connectivity observed in MccE492m isolated from bacterial cultures. Equivalent post-transfer acyl migration from the C3′ hydroxyl to the C2′ hydroxyl of ribose occurs in aminoacyl tRNA chemistry. Because of the C4′ to C6′ migration of the glycosyl ester in C_{10}E492-MGE, we sought to establish if 6-deoxyMGE (Scheme S1) is a substrate for MceIJ. We hypothesized that the protein complex would attach C_{10}E492 to the C4′ position of the 6-deoxyglucose moiety and that only one product, C_{10}E492-C4′-MGE, would be observed. MceIJ indeed accepts 6-deoxyMGE as a substrate (Figure 4); however, two products with catecholate absorption and the diagnostic *m/z* value were observed. We conclude that the first product peak corresponds to the C4′ glycosyl ester and that the second peak is an unanticipated and as yet uncharacterized structural isomer. Although this rearrangement is not physiologically significant, it indicates that initial attachment of C_{10}E492 at C4′ generates an unfavorable isomer and that migration to another site will occur even in the absence of the C6′ hydroxyl.

Acyl transfer via esterification of a Cys thiol residue is a common phenomenon, and we therefore chose to mutate the three Cys residues in MceI to alanines. Initial activity assays employing the C_{10}E492/MGE model system and MceI(C29A)J,

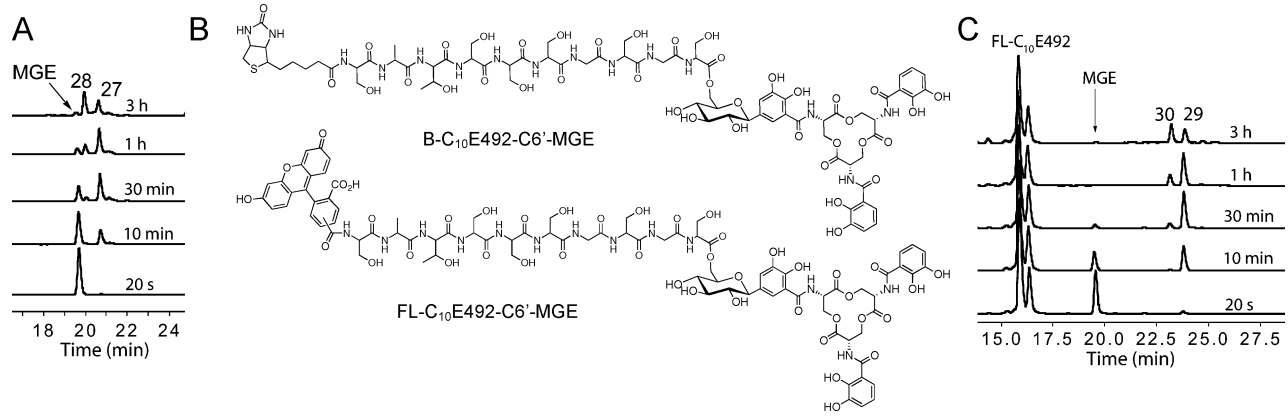

FIGURE 8: MceIJ accepts C_{10}E492 peptides with derivatized N-termini. (A) Time course (316 nm traces) for the MceIJ-catalyzed attachment of MGE to B-C_{10}E492. (B) Structures of B-C_{10}E492-C6′-MGE and FL-C_{10}E492-C6′-MGE. (C) Time course (440 nm traces) for the MceIJ-catalyzed attachment of MGE to FL-C_{10}E492. The FL-C_{10}E492 peptide is a mixture of the 5′ and 6′ isomers. Tables 2 and 3 list the *m*/*z* data and kinetic parameters, respectively.

MceI(C109A)J, or MceI(C110AJ) revealed that the mutants are active and there is no covalent acyl-S-MceI intermediate in the MceIJ-catalyzed reaction (Figure 3).

MceI shares weak homology with HlyC, the acyltransferase necessary for activation of hemolysin toxin (*45*). It catalyzes the fatty acid acylation of the ϵ-amino groups of lysine residues 564 and 690 in prohemolysin, requires acyl-acyl carrier protein as the acyl donor, and proceeds via an acyl-HlyC intermediate. Extensive site-directed mutagenesis of HlyC suggested formation of an acyl-His23 linkage during catalysis (*55, 56*). Such behavior is unusual because His residues are generally involved in acid−base chemistry and are rarely sites of acyl transfer, and because transfer of fatty acids generally proceeds via acyl-S-enzyme intermediates. Because of the weak homology between MceI and HlyC and the lack of an acyl-S-MceI intermediate, we chose to mutate the five His residues of MceI to Ala to determine if any are required for C_{10}-C4′-MGE formation. Each His mutant displayed activity in assays that employed the C_{10}E492/MGE model system and provided product distributions comparable to that of wild-type MceIJ (Figure 3), indicating that no His residue plays essential acid−base chemistry or provides an acyl-His-MceI intermediate. We conclude that MceI and HlyC do not share a common catalytic mechanism.

Selectivity studies revealed several important facets about MceIJ recognition of both siderophore and peptide substrates: (i) MceIJ accepts all glycosylated enterobactin derivatives produced by the MccE492 gene cluster; (ii) the ferric species $[Fe(MGE)]^{3-}$ and $[Fe(DGE)]^{3-}$ are substrates; (iii) the C-terminal decapeptides for the structurally related microcins H47, I47, and M are accepted; (iv) the C-terminal serine residue side chain is not required for attachment of the glycosylated siderophore; (v) functionalization of the N-terminal serine of C_{10}E492 is well tolerated. In total, these observations provide an understanding of the requirements for MceIJ recognition of both siderophore and peptide substrates.

MccE492m analogues with Glc-$DHBS_2$ and Glc-DHBS at the C-terminus were identified in bacterial cultures recently (*37*). Assuming MccE492-(Glc-$DHBS_2$) and MccE492-(Glc-DHBS) are not degradation products, two maturation pathways for these derivatives starting from MccE492 and MGE/lin-MGE are possible: (i) MceIJ-catalyzed attachment of MGE/lin-MGE to the MccE492 C-terminus followed by MceD-catalyzed hydrolysis or (ii) MceD-catalyzed hydrolysis of MGE/lin-MGE to Glc-$DHBS_2$ and Glc-DHBS and subsequent MceIJ-catalyzed attachment of Glc-$DHBS_2$/Glc-DHBS to MccE492. We previously reported evidence for the former route (*38*). To investigate the possibility of the latter pathway, incubations of MceIJ with C_{10}E492, ATP, and Glc-$DHBS_2$/Glc-DHBS were analyzed, and HPLC analysis indicated that both siderophores were transferred to C_{10}E492 (Figure 4). From consideration of *O*-phenylglycopyranosides, we presume that the C-glycosidic linkage and/or catechol of Glc-DHBS are minimal structural requirements for recognition.

MceIJ also accepts $[Fe(MGE)]^{3-}$ and $[Fe(DGE)]^{3-}$ in vitro (Figure S4), but it is most likely that the apo siderophores are the substrates in vivo because iron acquisition would occur following maturation and export. We place an upper limit of the K_M value for MGE and $[Fe(MGE)]^{3-}$ at 3 μM. This low K_M value may ensure that MGE gets efficiently coupled to MccE492 in the producer cytoplasm prior to microcin export.

Comparisons of the product distributions for MceIJ-catalyzed reactions involving C_{10}E492 and the various Ent derivatives reveal trends that depend on the cyclic or linear nature of the siderophore scaffold. When a substrate with the intact macrolactone is employed (apo/ferric MGE/DGE), two product peaks with 316 nm absorption and *m*/*z* values equivalent to [C_{10}E492 + siderophore − H_2O] are observed in the analytical HPLC trace, which are attributed to the C4′ and the rearranged C6′ glycosyl ester products. When the siderophore is linearized, three (lin-MGE, Glc-$DHBS_2$) or four (Glc-DHBS) product peaks with the product *m*/*z* values are observed. We presume that linearization results in the formation of the C4′ and C6′ glycosyl esters in addition to one or two novel structural isomers. Structural characterization of these putative isomers has not been undertaken, and the origin of this behavior is yet to be determined. In prior studies of the MceD-catalyzed hydrolysis of the macrolactone ring of C_{10}E492-C6′-MGE to form C_{10}E492-(Glc-$DHBS_2$) and C_{10}E492-(Glc-DHBS), no evidence for glycosyl ester from the C6′ position migration was observed. Likewise, we previously reported conversion of C_{10}E492-C6′-MGE to C_{10}E492-C4′-MGE is unfavorable in the pH 7−9 range. For both Glc-$DHBS_2$ and Glc-DHBS, we assign the initial and final product peaks in the HPLC traces to the C4′ and 6′

isomers. We tentatively conclude that the unknown isomers are of questionable physiological relevance.

Because MccE492 has 84 residues and MceIJ processed various decapeptides and the C_{10}-C_{15}E492 peptides with similar relative rates, we reasoned that C_{10}E492 analogues with functionalized N-termini could be employed in MceIJ-catalyzed reactions to prepare siderophore conjugates that might enable subsequent localization studies or provide new antibiotics. In accord with this notion, MceIJ transferred MGE to FL-C_{10}E492 and B-C_{10}E492, the former with similar catalytic efficiency as C_{10}E492 (Figures 8 and S5, Table 3). MceIJ is therefore useful for the chemoenzymatic synthesis of siderophore conjugates where the two functional units are linked by a C_{10} peptide fragment. Novel siderophore-antibiotic therapeutics are of interest for the treatment of bacterial infections via siderophore permease-mediated uptake through the outer membrane permeability barrier of pathogenic Gram-negative bacteria (*57*).

In closing, the proteins of the MccE492 gene cluster assemble a "Trojan horse" siderophore-antibiotic conjugate that makes use of a virulence factor to destroy susceptible bacteria that express siderophore receptors. The studies of mechanism and selectivity provide key insights into the requirements for MceIJ to recognize, derivatize, and couple the MccE492 C-terminus. How each of the MceI and MceJ subunits work together to catalyze such a unique posttranslational modification with glucose bridging a ribosomal and nonribosomal peptide is not yet clear. Understanding the precise roles of MceI and MceJ will require structural investigations, additional mutagenesis, and direct detection of reaction intermediates.

ACKNOWLEDGMENT

We thank Drs. Jay Read and Carl Balibar for helpful discussions.

SUPPORTING INFORMATION AVAILABLE

Cloning, overexpression, and purification of His_6 fusions of RmlA; preparation of 6-deoxyMGE; primers employed for the site-directed mutagenesis of MceI (Table S1); Scheme S1 and Figures S1−S5. This material is available free of charge via the Internet at http://pubs.acs.org.

REFERENCES

1. Duquesne, S., Destoumieux-Garzón, D., Peduzzi, J., and Rebuffat, S. (2007) Microcins, gene-encoded antibacterial peptides from enterobacteria. *Nat. Prod. Rep. 24*, 708–734.
2. Duquesne, S., Petit, V., Peduzzi, J., and Rebuffat, S. (2007) Structural and Functional Diversity of Microcins, Gene-Encoded Antibacterial Peptides from Enterobacteria. *J. Mol. Microbiol. Biotechnol. 13*, 200–209.
3. Severinov, K., Semenova, E., Kazakov, A., Kazakov, T., and Gelfand, M. S. (2007) Low-molecular-weight post-translationally modified microcins. *Mol. Microbiol. 65*, 1380–1394.
4. Li, Y.-M., Milne, J. C., Madison, L. L., Kolter, R., and Walsh, C. T. (1996) From Peptide Precursors to Oxazole and Thiazole-Containing Peptide Antibiotics: Microcin B17 Synthase. *Science 274*, 1188–1193.
5. Milne, J. C., Roy, R. S., Eliot, A. C., Kelleher, N. L., Wokhlu, A., Nickels, B., and Walsh, C. T. (1999) Cofactor Requirements and Reconstitution of Microcin B17 Synthetase: A Multienzyme Complex that Catalyzes the Formation of Oxazoles and Thiazoles in the Antibiotic Microcin B17. *Biochemistry 38*, 4768–4781.
6. Kelleher, N. L., Hendrickson, C. L., and Walsh, C. T. (1999) Posttranslational Heterocyclization of Cysteine and Serine Residues in the Antibiotic Microcin B17: Distributivity and Directionality. *Biochemistry 38*, 15623–15630.
7. Salomón, R. A., and Farías, R. N. (1992) Microcin 25, a Novel Antimicrobial Peptide Produced by *Escherichia coli*. *J. Bacteriol. 174*, 7428–7435.
8. Bellomio, A., Vincent, P. A., de Arcuri, B. F., Farías, R. N., and Morero, R. D. (2007) Microcin J25 has Dual and Independent Mechanisms of Action in *Escherichia coli*: RNA Polymerase Inhibition and Increased Superoxide Production. *J. Bacteriol. 189*, 4180–4186.
9. Rosengren, K. J., Clark, R. J., Daly, N. L., Göransson, U., Jones, A., and Craik, D. J. (2003) Microcin J25 Has a Threaded Sidechain-to-Backbone Ring Structure and Not a Head-to-Tail Cyclized Backbone. *J. Am. Chem. Soc. 125*, 12464–12474.
10. Bayro, M. J., Mukhopadhyay, J., Swapna, G. V. T., Huang, J. Y., Ma, L.-C., Sineva, E., Dawson, P. E., Montelione, G. T., and Ebright, R. H. (2003) Structure of Antibacterial Peptide Microcin J25: a 21-Residue Lariat Protoknot. *J. Am. Chem. Soc. 125*, 12382–12383.
11. Wilson, K.-A., Kalkum, M., Ottesen, J., Yuzenkova, J., Chait, B. T., Landick, R., Muir, T., Severinov, K., and Darst, S. A. (2003) Structure of Microcin J25, a Peptide Inhibitor of Bacterial RNA Polymerase, is a Lassoed Tail. *J. Am. Chem. Soc. 125*, 12475–12483.
12. Duquesne, S., Destoumieux-Garzón, D., Zirah, S., Goulard, C., Peduzzi, J., and Rebuffat, S. (2007) Two Enzymes Catalyze the Maturation of a Lasso Peptide in *Escherichia coli*. *Chem. Biol. 14*, 793–803.
13. Novoa, M. A., Díaz-Guerra, L., San Millán, J. L., and Moreno, F. (1986) Cloning and Mapping of the Genetic Determinants for Microcin C7 Production and Immunity. *J. Bacteriol. 168*, 1384–1391.
14. González-Pastor, J. E., San Millán, J. L., Castilla, M. Á., and Moreno, F. (1995) Structure and Organization of Plasmid Genes Required to Produce the Translation Inhibitor Microcin C7. *J. Bacteriol. 177*, 7131–7140.
15. Guijarro, J. I., González-Pastor, J. E., Baleux, F., San Millán, J. L., Castilla, M. A., Rico, M., Moreno, F., and Delepierre, M. (1995) Chemical Structure and Translation Inhibition Studies of the Antibiotic Microcin C7. *J. Biol. Chem. 270*, 23520–23532.
16. Roush, R. F., Nolan, E. M., Löhr, F., and Walsh, C. T. (2008) Maturation of an *Escherichia coli* Ribosomal Peptide Antibiotic by ATP-Consuming N-P Bond Formation in Microcin C7. *J. Am. Chem. Soc. 130*, 3603–3609.
17. Metlitskaya, A., Kazakov, T., Kommer, A., Pavlova, O., Praetorius-Ibba, M., Ibba, M., Krasheninnikov, I., Kolb, V., Khmel, I., and Severinov, K. (2006) Aspartyl-tRNA Synthetase is the Target of Peptide Nucleotide Antibiotic Microcin C. *J. Biol. Chem. 281*, 18033–18042.
18. Poey, M. E., Azpiroz, M. F., and Laviña, M. (2006) Comparative Analysis of Chromosome-Encoded Microcins. *Antimicrob. Agents Chemother. 50*, 1411–1418.
19. de Lorenzo, V. (1984) Isolation and characterization of microcin E492 from *Klebsiella pneumoniae*. *Arch. Microbiol. 139*, 72–75.
20. Pons, A.-M., Zorn, N., Vignon, D., Delalande, F., Dorsselaer, A. V., and Cottenceau, G. (2002) Microcin E492 is an Unmodified Peptide Related in Structure to Colicin V. *Antimicrob. Agents Chemother. 46*, 229–230.
21. Thomas, X., Destoumieux-Garzón, D., Peduzzi, J., Afonso, C., Blond, A., Birlirakis, N., Goulard, C., Dubost, L., Thai, R., Tabet, J.-C., and Rebuffat, S. (2004) Siderophore Peptide, a New Type of Post-translationally Modified Antibacterial Peptide with Potent Activity. *J. Biol. Chem. 279*, 28233–28242.
22. Raymond, K. N., Dertz, E. A., and Kim, S. S. (2003) Enterobactin: An archetype for microbial iron transport. *Proc. Natl. Acad. Sci. U.S.A. 100*, 3584–3588.
23. Bister, B., Bischoff, D., Nicholson, G. J., Valdebenito, M., Schneider, K., Winkelmann, G., Hantke, K., and Süssmuth, R. D. (2004) The structure of salmochelins: C-glucosylated enterobactins of *Salmonella enterica*. *BioMetals 17*, 471–481.
24. Luo, M., Lin, H., Fischbach, M. A., Liu, D. R., Walsh, C. T., and Groves, J. T. (2006) Enzymatic Tailoring of Enterobactin Alters Membrane Partitioning and Iron Acquisition. *ACS Chem. Biol. 1*, 29–32.
25. Goetz, D. H., Holmes, M. A., Borregaard, N., Bluhm, M. E., Raymond, K. N., and Strong, R. K. (2002) The Neutrophil Lipocalin NGAL is a Bacteriostatic Agent that Interferes with Siderophore-Mediated Iron Acquisition. *Mol. Cell 10*, 1033–1043.

26. Flo, T. H., Smith, K. D., Sato, S., Rodriguez, D. J., Holmes, M. A., Strong, R. K., Akira, S., and Aderem, A. (2004) Lipocalin 2 mediates an innate immune response to bacterial infection by sequestrating iron. *Nature 432*, 917–921.
27. Fischbach, M. A., Lin, H., Zhou, L., Yu, Y., Abergel, R. J., Liu, D. R., Raymond, K. N., Wanner, B. L., Strong, R. K., Walsh, C. T., Aderem, A., and Smith, K. D. (2006) The pathogen-associated iroA gene cluster mediates bacterial evasion of lipocalin 2. *Proc. Natl. Acad. Sci. U.S.A. 103*, 16502–16507.
28. Strahsburger, E., Baeza, M., Monasterio, O., and Lagos, R. (2005) Cooperative Uptake of Microcin E492 by Receptors FepA, Fiu, and Cir and Inhibition by the Siderophore Enterochelin and its Dimeric and Trimeric Hydrolysis Products. *Antimicrob. Agents Chemother. 49*, 3083–3086.
29. Destoumieux-Garzón, D., Peduzzi, J., Thomas, X., Djediat, C., and Rebuffat, S. (2006) Parasitism of iron-siderophore receptors of *Escherichia coli* by the siderophore-peptide microcin E492m and its unmodified counterpart. *BioMetals 19*, 181–191.
30. Lagos, R., Wilkens, M., Vergara, C., Cecchi, X., and Monasterio, O. (1993) Microcin E492 forms ion channels in phospholipid bilayer membranes. *FEBS Lett. 321*, 145–148.
31. Destoumieux-Garzón, D., Thomas, X., Santamaria, M., Goulard, C., Barthélémy, M., Boscher, B., Bessin, Y., Molle, G., Pons, A.-M., Letellier, L., Peduzzi, J., and Rebuffat, S. (2003) Microcin E492 antibacterial activity: evidence for a TonB-dependent inner membrane permeabilization on *Escherichia coli*. *Mol. Microbiol. 49*, 1031–1041.
32. Bieler, S., Silva, F., Soto, C., and Belin, D. (2006) Bactericidal Activity of both Secreted and Nonsecreted Microcin E492 Requires the Mannose Permease. *J. Bacteriol. 188*, 7049–7061.
33. Wilkens, M., Villanueva, J. E., Cofré, J., Chnaiderman, J., and Lagos, R. (1997) Cloning and Expression in *Escherichia coli* of Genetic Determinants for Production of and Immunity to Microcin E492 from *Klebsiella pneumoniae*. *J. Bacteriol. 179*, 4789–4794.
34. Lagos, R., Villanueva, J. E., and Monasterio, O. (1999) Identification and Properties of the Genes Encoding Microcin E492 and its Immunity Protein. *J. Bacteriol. 181*, 212–217.
35. Lagos, R., Baeza, M., Corsini, G., Hetz, C., Strahsburger, E., Castillo, J. A., Vergara, C., and Monasterio, O. (2001) Structure, organization and characterization of the gene cluster involved in the production of microcin E492, a channel-forming bacteriocin. *Mol. Microbiol. 42*, 229–243.
36. Corsini, G., Baeza, M., Monasterio, O., and Lagos, R. (2002) The expression of genes involved in microcin maturation regulates the production of active microcin E492. *Biochimie 84*, 539–544.
37. Vassiliadis, G., Peduzzi, J., Zirah, S., Thomas, X., Rebuffat, S., and Destoumieux-Garzón, D. (2007) Insight into siderophore-peptide biosynthesis: Enterobactin is a precursor for microcin E492 post-translational modification. *Antimicrob. Agents Chemother. 51*, 3546–3553.
38. Nolan, E. M., Fischbach, M. A., Koglin, A., and Walsh, C. T. (2007) Biosynthetic Tailoring of Microcin E492m: Post-translational Modification Affords an Antibacterial Siderophore-Peptide Conjugate. *J. Am. Chem. Soc. 129*, 14336–14347.
39. Fujiyama, A., Tsunasawa, S., Tamanoi, F., and Sakiyama, F. (1991) S-Farnesylation and Methyl Esterification of C-terminal Domain of Yeast RAS2 Protein Prior to Fatty Acid Acylation. *J. Biol. Chem. 266*, 17926–17931.
40. Scarrow, R. C., Ecker, D. J., Ng, C., Liu, S., and Raymond, K. N. (1991) Iron(III) Coordination Chemistry of Linear Dihydroxyserine Compounds Derived from Enterobactin. *Inorg. Chem. 30*, 900–906.
41. Heckman, K. L., and Pease, L. R. (2007) Gene splicing and mutagenesis by PCR-driver overlap extension. *Nat. Protocols 2*, 924–932.
42. Jiqing, J., Biggins, J. B., and Thorson, J. S. (2000) A General Enzymatic Method for the Synthesis of Natural and "Unnatural" UDP- and TDP-Nucleotide Sugars. *J. Am. Chem. Soc. 122*, 6803–6804.
43. McClelland, M., Sanderson, K. E., Spieth, J., Clifton, S. W., Latreille, P., Courtney, L., Porwollik, S., Ali, J., Dante, M., Du, F., Hou, S., Layman, D., Leonard, S., Nguyen, C., Scott, K., Holmes, A., Grewal, N., Mulvaney, E., Ryan, E., Suh, H., Florea, L., Miller, W., Stoneking, T., Nhan, M., Waterston, R., and Wlison, R. K. (2001) Complete genome sequence of *Salmonella enterica* servoar *Typhimurium* LT2. *Nature 413*, 852–856.
44. Fischbach, M. A., Lin, H., Liu, D. R., and Walsh, C. T. (2005) In vitro characterization of IroB, a pathogen-associated C-glycosyltransferase. *Proc. Natl. Acad. Sci. U.S.A. 102*, 571–576.
45. Trent, M. S., Worsham, L. M. S., and Ernst-Fonberg, M. L. (1998) The Biochemistry of Hemolysin Toxin Activation: Characterization of HlyC, an Internal Protein Acyltransferase. *Biochemistry 37*, 4644–4652.
46. Laviña, M., Gaggero, C., and Moreno, F. (1990) Microcin M47, a Chromosome-Encoded Microcin Antibiotic of *Escherichia coli*. *J. Bacteriol. 172*, 6586–6588.
47. Gaggero, C., Moreno, F., and Laviña, M. (1993) Genetic Analysis of Microcin H47 Antibiotic System. *J. Bacteriol. 175*, 5420–5427.
48. Haas, A. L., Warms, J. V. B., Hershko, A., and Rose, I. A. (1982) Ubiquitin-activating Enzyme. *J. Biol. Chem. 257*, 2543–2548.
49. Haas, A. L., Warms, J. V. B., and Rose, I. A. (1983) Ubiquitin Adenylate: Structure and Role in Ubiquitin Activation. *Biochemistry 22*, 4388–4394.
50. Taylor, S. V., Kelleher, N. L., Kinsland, C., Chiu, H.-J., Costello, C. A., Backstrom, A. D., McLafferty, F. W., and Begley, T. P. (1998) Thiamin Biosynthesis in *Escherichia coli*. *J. Biol. Chem. 273*, 16555–16560.
51. Xi, J., Ge, Y., Kinsland, C., McLafferty, F. W., and Begley, T. P. (2001) Biosynthesis of the thiazole moiety of thiamin in *Escherichia coli*: Identification of an acyldisulfide-linked protein-protein conjugate that is functionally analogous to the ubiquitin/E1 complex. *Proc. Natl. Acad. Sci. US.A. 98*, 8513–8518.
52. Soll, D., and Schimmel, P. (1974) in *The Enzymes*, Vol. 10, 3rd ed., Academic Press, New York.
53. Park, J.-H., Dorrestein, P. C., Zhai, H., Kinsland, C., McLafferty, F. W., and Begley, T. P. (2003) Biosynthesis of the Thiazole Moiety of Thiamin Pyrophosphate (Vitamin B1). *Biochemistry 42*, 12430–12438.
54. Lehmann, C., Begley, T. B., and Ealick, S. E. (2006) Structure of the *Escherichia coli* ThiS-ThiF Complex, a Key Component of the Sulfur Transfer System in Thiamin Biosynthesis. *Biochemistry 45*, 11–19.
55. Trent, M. S., Worsham, L. M. S., and Ernst-Fonberg, M. L. (1999) HlyC, the Internal Protein Acyltransferase that Activates Hemolysin Toxin: Role of Conserved Histidine, Serine, and Cysteine Residues in Enzymatic Activity as Probed by Chemical Modification and Site-Directed Mutagenesis. *Biochemistry 38*, 3433–3439.
56. Worsham, L. M. S., Trent, M. S., Earls, L., Jolly, C., and Ernst-Fonberg, M. L. (2001) Insights into the Catalytic Mechanism of HlyC, the Internal Protein Acyltransferase that Activates *Escherichia coli* Hemolysin Toxin. *Biochemistry 40*, 13607–13616.
57. Budzikiewicz, H. (2001) Siderophore-Antibiotic Conjugates Used as Trojan Horses Against *Pseudomonas aeruginosa*. *Curr. Top. Med. Chem. 1*, 73–82.

BI800826J